ISSN 0020-1685, Inorganic Materials, 2020, Vol. 56, No. 3, pp. 297–303. © Pleiades Publishing, Ltd., 2020.
Russian Text © The Author(s), 2020, published in Neorganicheskie Materialy, 2020, Vol. 56, No. 3, pp. 311–318.

Effect of Composition on the Dielectric Properties of $(1 - x)Ba(Ti_{0.75}Sn_{0.25})O_3 \cdot xPbTiO_3$ Solid Solutions

A. I. Spitsin[a], A. A. Bush[a, *], V. I. Kozlov[a], A. V. Stepanov[a], K. E. Kamentsev[a], and E. A. Tishchenko[b, c]

[a] *MIREA—Russian Technological University, pr. Vernadskogo 78, Moscow, 119454 Russia*

[b] *Kapitza Institute for Physical Problems, Russian Academy of Sciences, ul. Kosygina 2, Moscow, 117339 Russia*

[c] *Peoples' Friendship University of Russia, ul. Ordzhonikidze 3, Moscow, 117198 Russia*

**e-mail: aabush@yandex.ru*

Received March 5, 2019; revised June 5, 2019; accepted June 17, 2019

Abstract—$(1 - x)Ba(Ti_{0.75}Sn_{0.25})O_3 \cdot xPbTiO_3$ ($0 \le x \le 1$) samples prepared by a standard ceramic processing route have been characterized by X-ray diffraction, thermogravimetry, and dielectric, piezoelectric, and pyroelectric measurements. The results demonstrate that the system in question contains solid solutions with the perovskite structure, which have cubic symmetry for $x < 0.2$ and tetragonal symmetry for $x \ge 0.2$. Increasing the percentage of $PbTiO_3$ in the samples has been shown to cause sequential changes in their dielectric properties in the following sequence: ferroelectric relaxor, reentrant ferroelectric relaxor, ferroelectric with a diffuse phase transition, and conventional ferroelectric.

Keywords: ferroelectric ceramics, solid solutions, X-ray diffraction analysis, dielectric properties, dielectric relaxation, phase transitions

DOI: 10.1134/S0020168520020168

INTRODUCTION

Since their properties are of both scientific and practical interest, solid solutions based on ferroelectric barium titanate, $BaTiO_3$ are the subject of intense studies and find wide practical application [1, 2]. In particular, it is well documented [1–11] that $Ba(Ti_{1-y}Sn_y)O_3$ (BTSn) solid solutions have high dielectric permittivity ε, a low dielectric loss tangent tan δ, high dielectric nonlinearity, and a good resistance to high electrical voltages, so they are employed in the fabrication of capacitors, varicaps, dynamic random access memory devices, and electric-field-controlled microwave devices (phase shifters, filters, antennas, etc.). Varying the composition of BTSn, one can tune the electric transport properties of the solid solutions over a wide range, optimizing them for particular applications.

Because of the proximity of the Curie point T_C of the BTSn materials to room temperature, they have a relatively large temperature coefficient of their dielectric permittivity and low spontaneous polarization P_s, which is a serious drawback in a number of applications. Since the $PbTiO_3$ (PT) phase, isostructural with barium titanate, exhibits pronounced ferroelectric properties and has high T_C (490°C) [1, 2], it is reasonable to expect that increasing the percentage of PT in $(1 - x)$BTSn $\cdot xPT$ solid solutions will raise their T_C, P_s, and piezoelectric parameters, with their good dielectric characteristics retained.

There is rather little published data on the properties of the $(1 - x)$BTSn $\cdot xPT$ materials, limited to results for the constituent binaries BTSn [1–11], $(Ba_{1-u}Pb_u)TiO_3$ [1, 2], and $(1 - x)$BSn $\cdot xPT$ [12, 13]. In previous work, neither the phase diagram of the barium titanate–barium stannate–lead titanate ternary system nor properties of solid solutions existing in it have been systematically studied.

In this paper, we report the preparation of new ferroelectric solid solutions with the perovskite structure, $(1 - x)Ba(Ti_{0.75}Sn_{0.25})O_3 \cdot xPbTiO_3$, over the entire composition range $0 \le x \le 1$; their structural, dielectric, piezoelectric, and pyroelectric properties; and the influence of chemical composition and synthesis, heat treatment, and poling conditions on their properties.

EXPERIMENTAL PROCEDURE AND RESULTS

Preparation of ceramics. Samples of the $BaTiO_3$–$BaSnO_3$–$PbTiO_3$ (BT–BSn–PT) ternary system were prepared in air by solid-state reactions via standard ceramic processing route. We used the following starting chemicals: TiO_2 (extrapure grade), SnO_2 (pure grade), PbO (analytical grade), and $BaCO_3$ (analytical grade). The compositions of the synthesized samples corresponded to

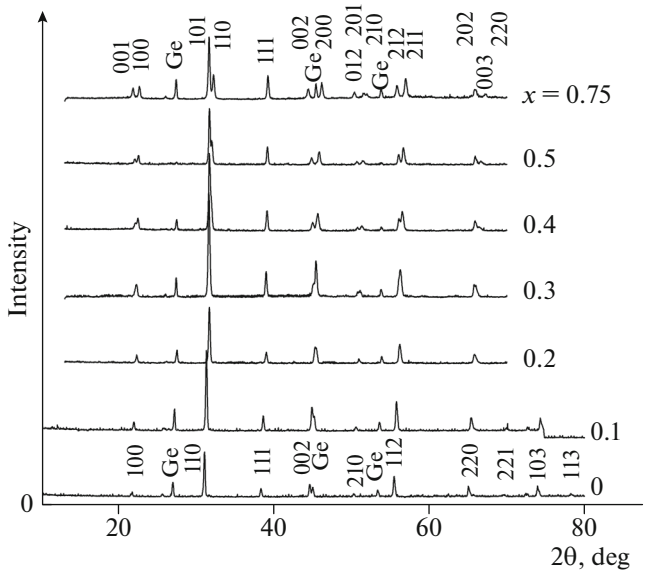

Fig. 1. X-ray diffraction patterns of powdered synthesized $(1 - x)Ba(Ti_{0.75}Sn_{0.25})O_3 \cdot xPbTiO_3$ samples.

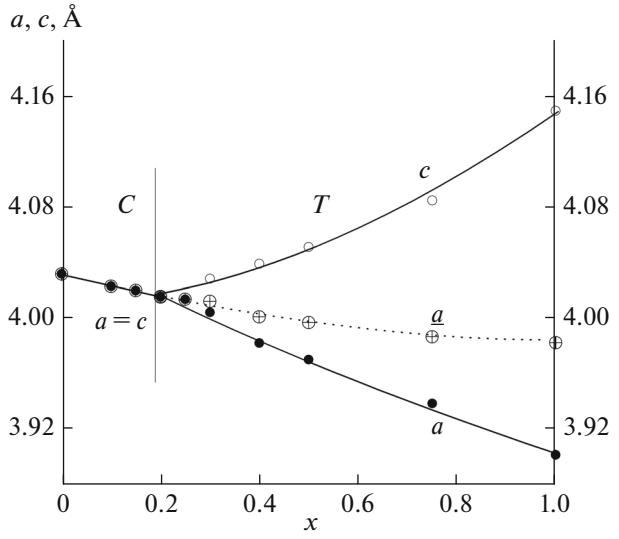

Fig. 2. Composition dependences of the unit-cell parameters a and c for the $(1 - x)Ba(Ti_{0.75}Sn_{0.25})O_3 \cdot xPbTiO_3$ solid solutions ($\underline{a} = V^{1/3}$ is the reduced unit-cell parameter; C, cubic symmetry; T, tetragonal symmetry).

the general formula $(1 - x)Ba(Ti_{0.75}Sn_{0.25})O_3 \cdot xPbTiO_3$ with $0 \le x \le 1$. Appropriate mixtures of these chemicals were homogenized by grinding with ethanol in an agate mortar. The homogenized mixtures were fired for 8 h in an SNOL 12/16 electric compartment furnace with several intermediate coolings and grindings of the firing products. The firing temperature of the $x = 0$ mixture was 1450°C. With increasing PT (lower melting point component) concentration in the samples, the firing temperature was lowered to 1250°C. Higher synthesis temperatures at low PT concentrations were needed because, according to X-ray diffraction analysis data, the $x = 0$ samples synthesized at 1270°C consisted of a mixture of the $BaTiO_3$ and $BaSnO_3$ phases. Single-phase samples with this composition were obtained when the synthesis temperature was raised to 1450°C.

The synthesis products were ground and pressed at ≈150 atm into cylindrical green compacts ≈10 mm in diameter and 1–3 mm in thickness, which were then sintered between 1250 and 1450°C for 2–4 h. As a result, we obtained ceramic samples ranging in density from 80 to 95% of theoretical density. Electrical contacts for dielectric measurements were made on the faces of the ceramic disks by firing Ag-containing paste.

X-ray diffraction characterization and thermogravimetric analysis. The phase composition of the samples was determined by X-ray diffraction on a DRON-4 computer-controlled X-ray diffractometer (filtered copper radiation), using powdered Ge crystals as an internal standard. The position and intensities of reflections in the X-ray diffraction patterns of the ceramic samples (Fig. 1) were consistent with those expected for $BaTiO_3$-, $BaSnO_3$-, and $PbTiO_3$-based solid solutions with the perovskite structure [14]. All of the reflections present in the X-ray diffraction patterns of the samples could be indexed in a cubic or tetragonal unit cell with $a \approx c \approx 4$ Å. Thus, the samples consisted of solid solutions with the perovskite structure. Figure 2 shows composition dependences of the unit-cell parameters determined by indexing the X-ray diffraction patterns of the solid solutions. With increasing PT content, the reduced unit-cell parameter of the solid solutions decreases almost linearly (Fig. 2), which is obviously due to the substitution of Pb^{2+}, smaller cations (1.19 Å) [15], for Ba^{2+} cations (1.35 Å) in the perovskite structure.

It follows from the peak positions in the X-ray diffraction patterns that, to a first approximation, the solid solutions containing less than 30 mol % PT have cubic symmetry, whereas the solid solutions with $x \ge 0.30$ have tetragonal symmetry. However, since the Curie temperature of the samples with $x = 0.20$ and 0.25 exceeds room temperature (see below), their actual symmetry at room temperature is tetragonal rather than cubic. That the X-ray diffraction patterns of these samples can be indexed in cubic symmetry is obviously due to the low degree of tetragonal distortion of the cubic crystal structure of the solid solutions with these compositions. Thus, taking into account the Curies temperatures of the solid solutions. we conclude that they undergo a polymorphic phase transition from cubic to tetragonal symmetry near $x \approx 0.18$. To more accurately determine structural parameters of the solid solutions near the polymorphic phase boundary and find out whether perovskite solid solutions differing in symmetry can coexist in this region,

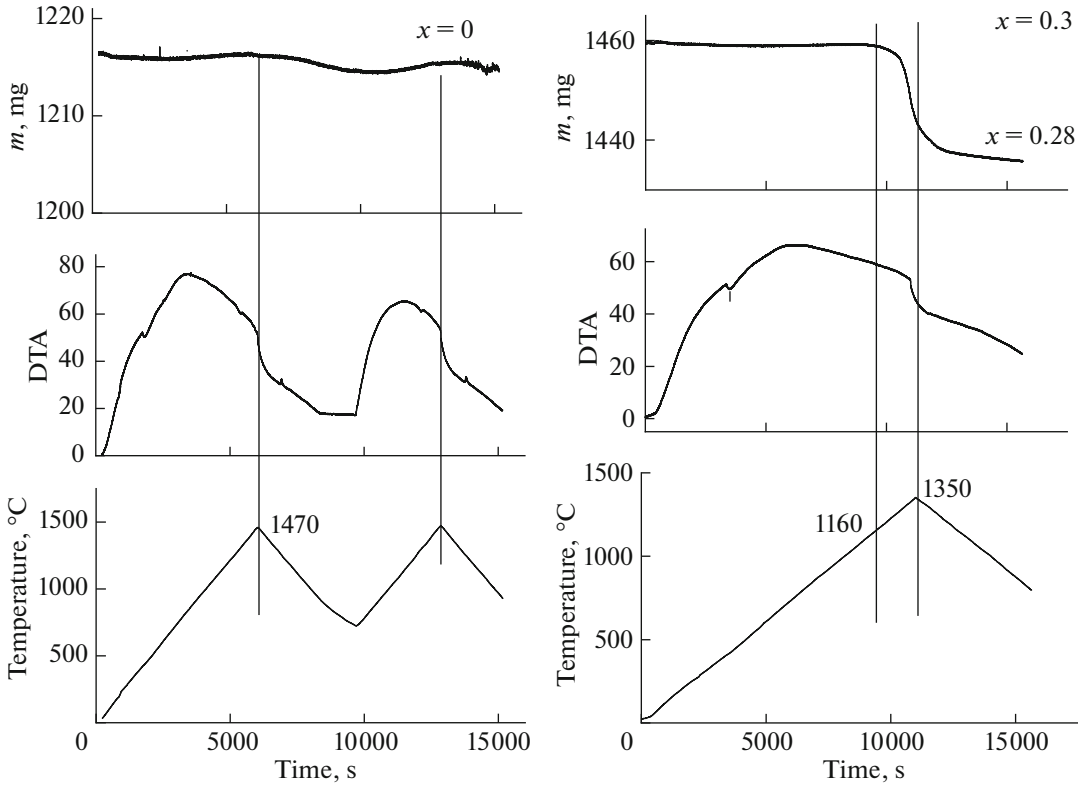

Fig. 3. Thermal analysis results for powdered samples with $x = 0$ and 0.30.

X-ray structure analysis of the samples by the Rietveld method is needed.

Thermogravimetric analysis was carried out with a Q-1500 Paulik–Paulik–Erdey thermoanalytical system. The results are presented in Fig. 3. It is seen that the weight loss of the PT-free sample during heating to 1470°C is <0.1%. It is thus reasonable to conclude that, in the course of the synthesis of such samples, their stoichiometric composition remains essentially unchanged. Heating the Pb-containing samples to above 1160°C leads to a marked weight loss (~2 wt %), which is obviously due to PbO volatility. As the 0.7BTSn · 0.3PT sample is heated to 1340°C, its composition changes to 0.7BTSn · 0.28PT, as a result of the lead oxide release. Because of this, the starting mixtures for the preparation of the ceramics were packed in Pb-containing powder.

Dielectric properties. Dielectric measurements were performed at temperatures from 100 to 800 K and frequencies from 25 Hz to 1 MHz using an E7-20 LCR meter. The results are presented in Figs. 4 and 5.

It is found that, at PT contents in the range 0–10 mol % $PbTiO_3$, the $\varepsilon(T, f)$ curves have a single detectable peak, whose position T_{max} shifts to higher temperatures with increasing frequency, suggesting that the solid solutions in this composition range are ferroelectric relaxors (FE-Rs), which typically exhibit such behavior [16]. The $T_{max}(f)$ data for the $x = 0$ sample follow the Vogel–Fulcher phenomenological law $f = f_0\exp\{-E_a[k_B(T_m(f) - T_{VF})]\}$, where f_0 is the attempt frequency for surmounting a potential barrier of height E_a, k_B is Boltzmann's constant, and T_{VF} is the Vogel–Fulcher temperature, which in the case of lead magnesium niobate (PMN), a canonical relaxor, is related in the literature to the freezing of electric dipole dynamics and a transition from an ergodic ferroelectric relaxor state to a nonergodic one [16]. That the $x = 0$ material is a ferroelectric relaxor has been clearly demonstrated by different groups in a large number of reports [3, 4, 6, 7, 16, 17]. Clearly, the $(1 - x)Ba(Ti_{0.75}Sn_{0.25})O_3 \cdot xPbTiO_3$ solid solutions with low $PbTiO_3$ concentrations are also ferroelectric relaxors.

Unlike in the case of classic ferroelectric relaxors, such as $PbMg_{1/3}Nb_{2/3}O_3$ [16], the ferroelectric relaxor properties of the $(1 - x)$BTSn · xPT solid solutions result from isovalent, rather than heterovalent, substitutions in the A and B sublattices of the perovskite structure, without nominal charge disorder. The ferroelectric relaxor properties of these materials are most likely due to competing interactions that result in long-range ferroelectric order or disorder in the arrangement of the $[TiO_6]$ polar and $[SnO_6]$ nonpolar octahedral groups, as well as in the correlated or uncorrelated displacements of the Pb^{2+} cations, with an unshared $6s^2$ electron pair, from symmetric sites in the crystal structure of $(1 - x)$BTSn · xPT [16, 17].

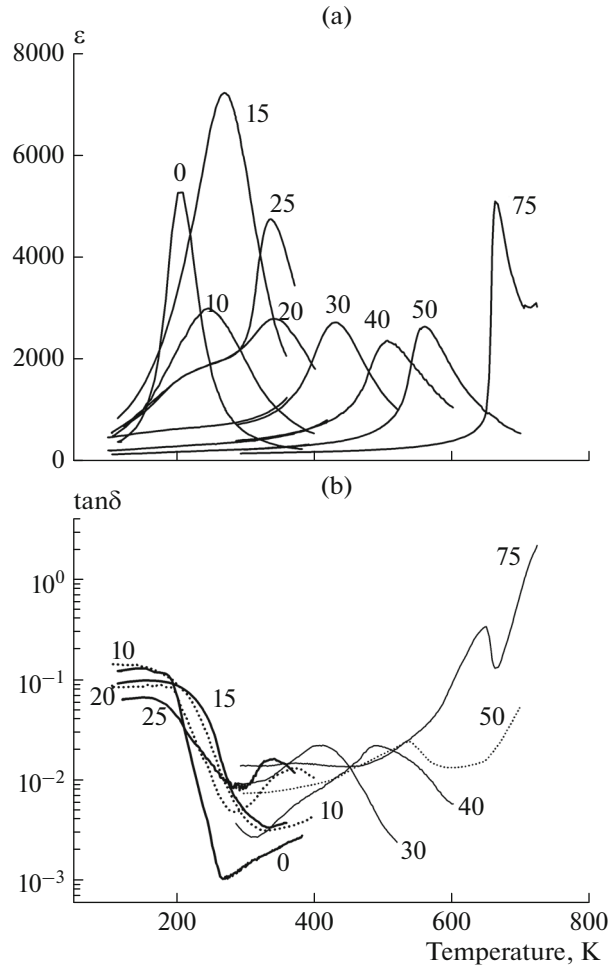

Fig. 4. $\varepsilon(T)$ and $\tan\delta(T)$ curves at a frequency $f = 100$ kHz for the $(1-x)Ba(Ti_{0.75}Sn_{0.25})O_3 \cdot xPbTiO_3$ ceramics. The numbers at the curves specify the value of $100x$.

In the composition range $0.10 < x < 0.30$, the $\varepsilon(T, f)$ curves have two maxima: a lower temperature, frequency-dependent peak of the relaxor type in the range 190–250 K and a higher temperature peak in the range 270–340 K, whose position is frequency-independent. The higher temperature peak is due to the ferroelectric phase transition in the solid solutions. Its temperature obviously corresponds to the Curie temperature of the ferroelectric solid solutions, as supported by pyroelectric measurement results.

The relaxation peaks observed at $T_{max} < T_C$ in the $\varepsilon(T)$ and $\tan\delta(T)$ curves of the solid solutions in the range $0.10 < x < 0.30$ originate from the analogous maxima of the $x = 0$ ferroelectric relaxor on the addition of the PT component. It is, therefore, reasonable to conclude that these solid solutions also have ferroelectric relaxor properties below their T_C. This conclusion is supported as well by the fact that the $T_{max}(f)$ data for the $x = 0.20$ sample follows the Vogel–Fulcher law (Fig. 5) with f_0, E_a, and T_{VF} parameters characteristic of ferroelectric relaxors ($f_0 = 4.2 \times 10^{10}$ Hz, $E_a = 0.014(10)$ eV, and $T_{VF} = 183(4)$ K). Unlike conventional ferroelectric relaxors [16], the solid solutions in the composition range in question exhibit relaxor behavior below, rather than above, their ferroelectric Curie temperature (as seen in Fig. 5); that is, first, an ordered ferroelectric state is formed in them, and then, as the temperature is lowered, the material returns to a disordered, relaxor state. Such behavior is characteristic of so-called reentrant ferroelectric relaxors (R-FE-R) [17, 18].

The assumption that below T_C, the materials under consideration have conventional relaxation maxima arising, for example, from inhomogeneities at grain boundaries of the ceramic or at material/electrode interfaces or from the dynamics of ferroelectric domain walls or lead and oxygen vacancies, inherent in Pb-containing oxide phases, is inconsistent with the fact that the samples with $x \geq 0.30$ prepared by the same process have no such anomalies. Moreover, the $\tan\delta(T)$ curve has not single maxima, characteristic of conventional relaxation processes, but plateau-like low-temperature maxima, characteristic of ferroelectric relaxors, in which the relaxation process involves not individual dipoles, but clusters of dipoles with a wide range of relaxation times [16, 17].

In the composition range $0.30 \leq x \leq 1$, the $\varepsilon(T, f)$ data has one, frequency-independent, well-defined maximum, whose position shifts to higher temperatures with increasing PT concentration (Figs. 4, 5). Clearly, this peak arises from the ferroelectric phase transition of the solid solutions. With increasing PT concentration in the solid solutions, their Curie temperature rises from 270 K at $x = 0.15$ to 763 K at $x = 1$. This is accompanied by a gradual reduction in the width of the dielectric permittivity peak in the region of their Curie temperature and, accordingly, by a change in their dielectric properties: from ferroelectric properties with a diffuse phase transition (FE DPT) to conventional ferroelectric (FE) properties, similar to those of $PbTiO_3$.

Thus, increasing the percentage of $PbTiO_3$ in the solid solutions under investigation leads to a change in their dielectric properties from ferroelectric relaxor properties to ferroelectric ones at $PbTiO_3$ concentrations above 25 mol %. In the intermediate composition range $0.1 < x < 0.3$, the properties of the solid solutions are characteristic of reentrant ferroelectric relaxors.

Figure 6a shows composition dependences of peak temperatures in the temperature dependence of dielectric permittivity for the solid solutions under investigation. The maxima in d_{33} and ε are located at different compositions (at $x = 0.25$ and 0.15, respectively), which can probably be accounted for by the fact that they are influenced by not only the proximity of the composition to the polymorphic phase bound-

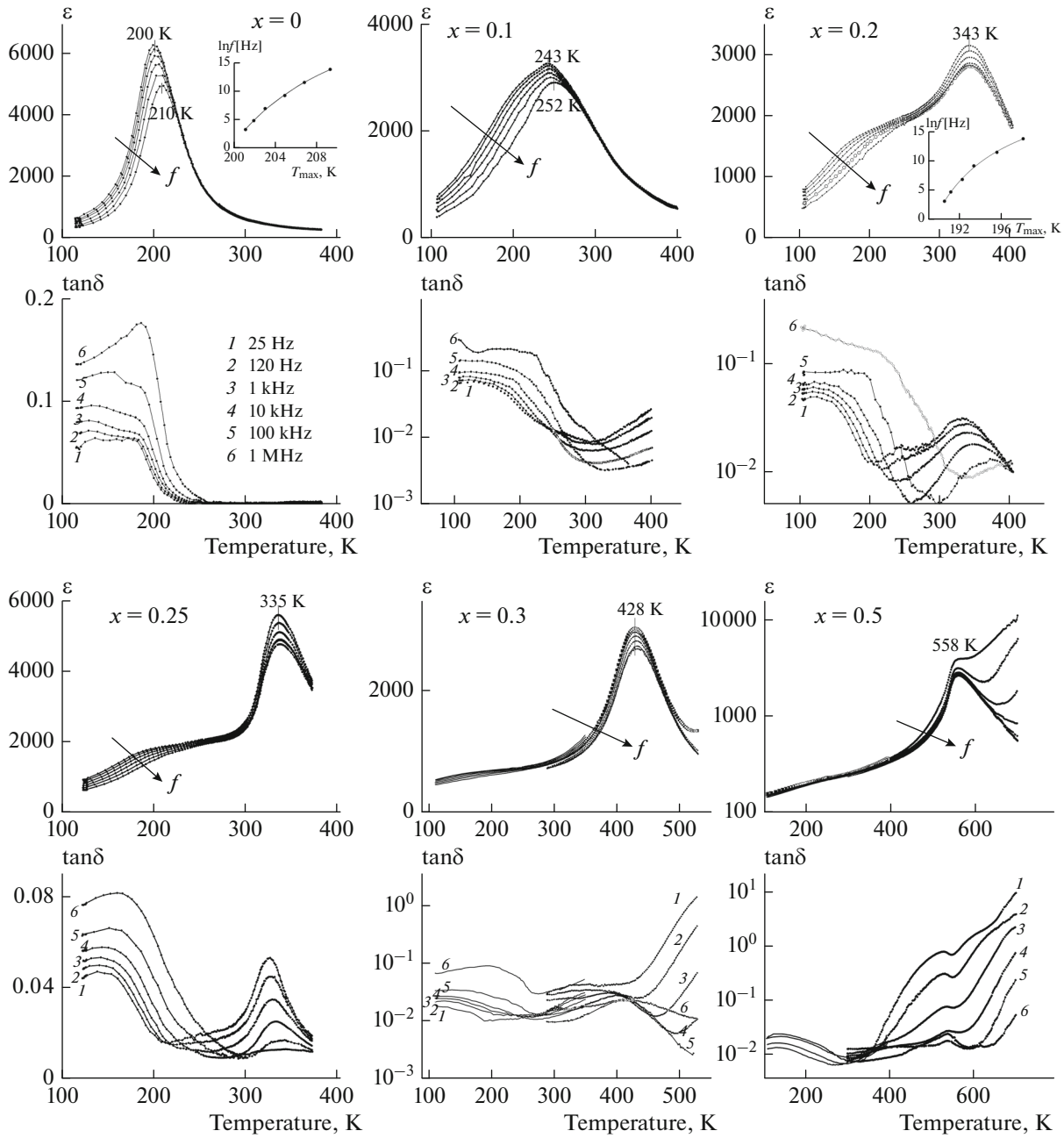

Fig. 5. ε(T) and tan δ(T) curves at different frequencies for the $(1-x)Ba(Ti_{0.75}Sn_{0.25})O_3 \cdot xPbTiO_3$ samples with $x = 0$–0.50. Insets: $T_{max}(f)$ curves and fits to the Vogel–Fulcher formula. The symbols represent the experimental data and the lines represent the fits.

ary, but also other factors: the degree of poling and porosity of the ceramic samples.

The increase in T_C and the absence of low-temperature anomalies in the ε(T) and tan δ(T) curves at $PbTiO_3$ concentrations above 25 mol % improve the thermal stability of the dielectric characteristics of the solid solutions near room temperature, which is of interest for practical applications. Also shown in Fig. 6b are composition dependences of the maximum dielectric permittivity in the ε(T) dependence.

Piezoelectric properties and thermally stimulated depolarization currents. The d_{33} piezoelectric coefficient of poled samples was determined near room temperature using an oscillating mechanical load method and a d_{33} meter (the United States). The measurement results are presented in Fig. 6b. The maximum piezoelectric coefficient (170 pC/N) is observed for the $x =$

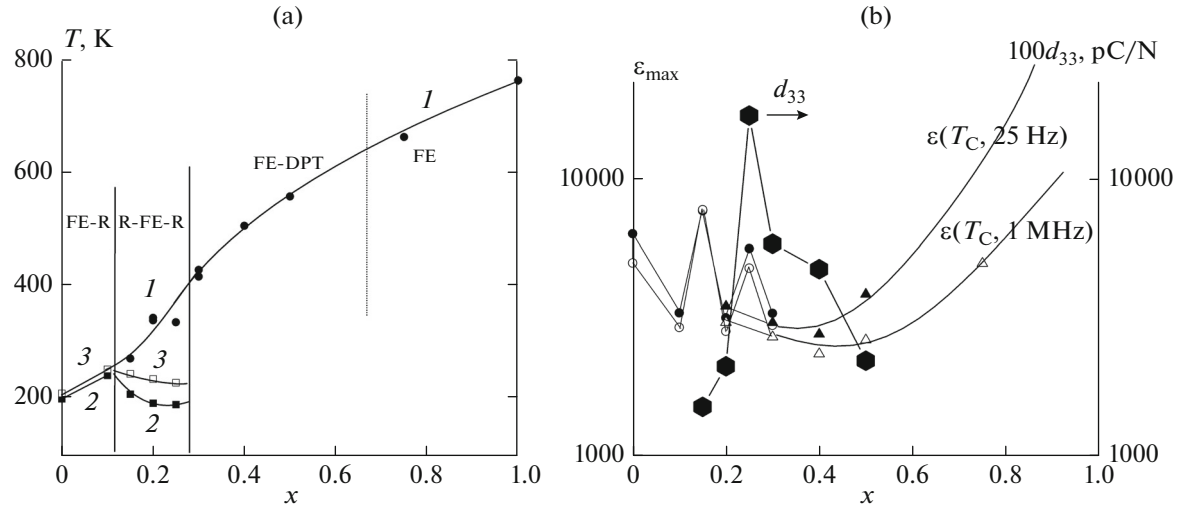

Fig. 6. Composition dependences of the Curie temperature (*1*), temperatures of the relaxation peaks in the ε(*T*) curves at *f* = 25 Hz (*2*) and *f* = 1 MHz (*3*) (a), piezoelectric modulus d_{33}, and maximum dielectric permittivity in its temperature dependence measured at *f* = 25 Hz and *f* = 1 MHz (b).

0.25 sample, which is obviously due to the proximity of its composition to the position of the polymorphic phase boundary found by us in the solid solution system under study.

Short-circuit thermally stimulated depolarization currents (TSDCs) were measured as a function of temperature using a V7-30 electrometer, whose input was connected to electrodes of a crystal. The measurements were performed during heating at a rate of ~0.1 K/s after poling. The samples were poled with an applied electric field $E_p \approx 1.0$ kV/cm during cooling from 470 to 90 K. The measurement results are presented in Fig. 7 in the form of temperature dependences of the TSDC normalized to the electrode area *S* and heating rate $dT/d\tau$. If a major contribution to the measured current is made by the pyroelectric effect, the TSDC thus normalized is the pyroelectric coefficient of the samples: $p^\sigma = (\partial P_s/\partial T)_\sigma$, where P_s is the spontaneous polarization of the samples and σ is mechanical stress.

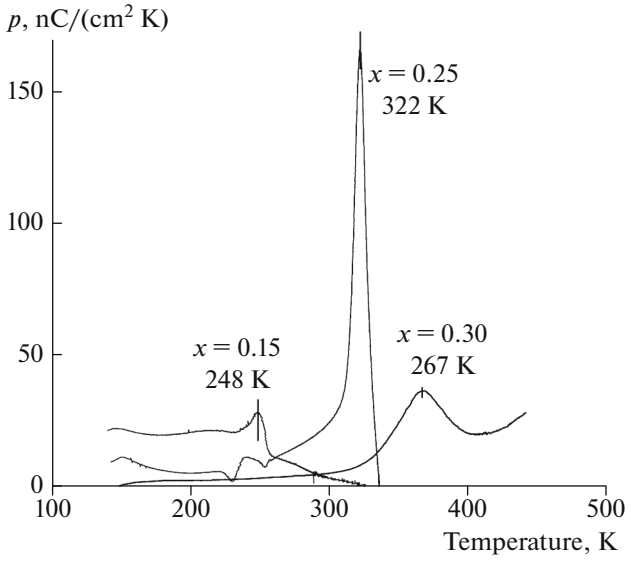

Fig. 7. Temperature dependences of the TSDC for the $(1-x)Ba(Ti_{0.75}Sn_{0.25})O_3 \cdot xPbTiO_3$ solid solutions after cooling of the samples in an electric field of ~1 kV/cm.

The TSDC through the poled samples of the solid solutions with tetragonal symmetry has well-defined maxima in the temperature range of the high-temperature maxima in the ε(*T*) curve. Above these temperatures (T_{mp}), the TSDC decreases. The fact that, below T_{mp}, the sign of the TSDC depends on the temperature scan direction suggests that it has a pyroelectric nature. These data leads us to conclude that the high-temperature maxima in the ε(*T*) curve of the tetragonal solid solutions are due to a ferroelectric phase transition and that, accordingly, the position of these maxima determines the Curie temperature of the solid solutions.

In addition, the temperature dependences of the TSDC through the samples have local extrema below T_{mp} (Fig. 7), where neither ε(*T*) nor tan δ(*T*) has noticeable features. The extrema possibly originate from a thermally stimulated discharge of electret charges produced during the poling of the samples or from the manifestation of the complex dynamics of the freezing of polar regions in the ferroelectric relaxor solid solutions.

CONCLUSIONS

$(1-x)Ba(Ti_{0.75}Sn_{0.25})O_3 \cdot xPbTiO_3$ ceramic samples in the $BaTiO_3$–$BaSnO_3$–$PbTiO_3$ ternary system have been prepared by solid-state reactions. According

to X-ray diffraction results, the samples consist of solid solutions with the perovskite structure.

The samples have been characterized by thermogravimetric analysis, and the variation in their composition due to the lead oxide volatility at high temperatures has been assessed.

We have obtained composition dependences of the symmetry and unit-cell parameters of the solid solutions. It has been shown that, at room temperature, the solid solution system studied has a cubic/transition polymorphic phase boundary in the $x \approx 0.18$ region: the solid solutions with $x < 0.20$ have cubic symmetry and those with $x \geq 0.20$ have tetragonal symmetry.

Temperature and frequency dependences of the dielectric permittivity ε and dielectric loss tangent tan δ for the solid solutions have been obtained at temperatures from 100 to 800 K and frequencies from 25 Hz to 1 MHz, and their Curie temperature T_C and characteristic temperatures of relaxation maxima, T_{max}, have been determined. Increasing the percentage of PT in the samples has been shown to cause changes in their dielectric properties in the following sequence: ferroelectric relaxor, reentrant ferroelectric relaxor, ferroelectric with a diffuse phase transition, and conventional ferroelectric similar in properties to $PbTiO_3$. In addition, with increasing $PbTiO_3$ content the T_C of the samples rises from 270 K at $x = 0.15$ to 763 K at $x = 1$.

We have studied the piezo- and pyroelectric properties of the solid solutions. The results demonstrate that the largest d_{33} piezoelectric coefficient is offered by the $x = 0.25$ solid solution, which is tentatively attributed to the proximity of its composition to the position of the polymorphic phase boundary in the system studied.

FUNDING

This work was supported by the Russian Federation Ministry of Science and Higher Education, project nos. 3.1099.2017/PCh and 3.4627.2017/VU.

ACKNOWLEDGMENTS

The measurements in this study were performed using equipment at the Shared Research Facilities Center, MIREA—Russian Technological University.

REFERENCES

1. Venevtsev, Yu.N., Politova, E.D., and Ivanov, S.A., *Segnetoelektriki i antisegnetoelektriki semeistva titanata bariya* (Ferroelectrics and Antiferroelectrics of the Barium Titanate Family), Moscow: Khimiya, 1985.
2. Rotenberg, B.A., *Keramicheskie kondensatornye dielektriki* (Ceramic Capacitor Dielectrics), St. Petersburg: Tipografiya OAO NII Girikond, 2000.
3. Zhang, Q., Zhai, J., and Kong, L.B., Relaxor ferroelectric materials for microwave tunable applications, *J. Adv. Dielectr.,* 2012, vol. 2, no. 1, paper 1 230 002.
4. Lu, S.G., Xu, Z.K., and Chena, H., Tunability and relaxor properties of ferroelectric barium stannate titanate ceramics, *Appl. Phys. Lett.,* 2004, vol. 85, no. 22, pp. 2319–2321.
5. Wei, X. and Yao, X., Preparation, structure and dielectric property of barium stannate titanate ceramics, *Mater. Sci. Eng., B,* 2007, vol. 137, nos. 1–3, pp. 184–188.
6. Lei, C., Bokov, A.A., and Ye, Z.-G., Ferroelectric to relaxor crossover and dielectric phase diagram in the $BaTiO_3$–$BaSnO_3$ system, *J. Appl. Phys.,* 2007, vol. 101, no. 8, paper 084 105.
7. Shvartsman, V.V., Dec, J., Xu, Z.K., Banys, J., Keburis, P., and Kleemann, W., Crossover from ferroelectric to relaxor behavior in $BaTi_{1-x}Sn_xO_3$ solid solutions, *Phase Transitions,* 2008, vol. 81, nos. 11–12, pp. 1013–1021.
8. Markovic, S., Jovalekic, C., Veselinovic, L., Mentus, S., and Uskokovic, D., Electrical properties of barium titanate stannate functionally graded materials, *J. Eur. Ceram. Soc.,* 2010, vol. 30, no. 6, pp. 1427–1435.
9. Xie, L., Li, Y.L., Yu, R., Cheng, Z.Y., Wei, X.Y., Yao, X., Jia, C.L., Urban, K., Bokov, A.A., Ye, Z.-G., and Zhu, J., Static and dynamic polar nanoregions in relaxor ferroelectric $Ba(Ti_{1-x}Sn_x)O_3$ system at high temperature, *Phys. Rev. B: Condens. Matter Mater. Phys.,* 2012, vol. 85, paper 014 118.
10. Deluca, M., Stoleriu, L., Curecheriu, L.P., et al., High-field dielectric properties and Raman spectroscopic investigation of the ferroelectric-to-relaxor crossover in $BaSn_xTi_{1-x}O_3$ ceramics, *J. Appl. Phys.,* 2012, vol. 111, no. 8, paper 084 102.
11. Yao, Y., Zhou, C., Lv, D., Wang, D., Wu, H., Yang, Y., and Ren, X., Large piezoelectricity and dielectric permittivity in $BaTiO_3 \cdot xBaSnO_3$ system: the role of phase coexisting, *Europhys. Lett.,* 2012, vol. 98, no. 2, paper 27 008.
12. Han, X., Li, X., Long, X., He, H., and Cao, Y., A dielectric and ferroelectric solid solution in $(10x)BaSnO_3$–$xPbTiO_3$ with morphotropic phase boundary, *J. Mater. Chem.,* 2009, vol. 19, no. 34, pp. 6132–6136.
13. Wang, Z., Li, X., Xe, C., and Long, X., Relaxor behavior in the $(1-x)BaSnO_3$–$xPbTiO_3$ solid solution, *Solid State Commun.,* 2011, vol. 151, no. 4, pp. 329–331.
14. *Powder Diffraction Files of the International Centre for Diffraction Data (ICDD)*, 1999.
15. Shannon, R.D., Revised effective ionic radii and systematic studies of interatomic distances in halides and chalcogenides, *Acta Crystallogr., Sect. A: Cryst. Phys., Diffr., Theor. Gen. Crystallogr.,* 1976, vol. 32, no. 5, pp. 751–767.
16. Bokov, A.A. and Ye, Z.-G., Recent progress in relaxor ferroelectrics with perovskite structure, *J. Mater. Sci.,* 2006, vol. 41, no. 1, pp. 31–52.
17. Shvartsman, V.V. and Lupescu, D.C., Lead-free relaxor ferroelectrics, *J. Am. Ceram. Soc.,* 2012, vol. 95, no. 1, pp. 1–26.
18. Bokov, A.A. and Ye, Z.-G., *Reentrant phenomena in relaxors, Nanoscale Ferroelectrics and Multiferroics: Key Processing and Characterization Issues, and Nanoscale Effects,* Alguerro, M., Gregg, J.M., and Mitoseriu, L., Eds., New York: Wiley, 2016, 1st ed., chapter 23, pp. 729–764.